Advances in Monitoring and Interventions for Emerging Infectious Diseases

An Expert Insights publication

Emerging infectious disease is a rising area of focus for global health. This publication provides Expert Insights into recent advances in infectious disease research that can be accomplished using advanced flow cytometry, ligand binding antibody assays and live-cell analysis approaches offered by Sartorius.

Free Download

Giancarlo Ceccarelli   ORCID iD: 0000-0001-5921-3180

Massimo Ciccozzi   ORCID iD: 0000-0003-3866-9239

carolina scagnolari   ORCID iD: 0000-0003-1044-1478

The crosstalk between gut barrier impairment, mitochondrial dysfunction and microbiota alterations in people living with HIV

Letizia Santinelli [1], Giacomo Rossi [2], Giorgia Gioacchini [3], Ranieri Verin [4], Luca Maddaloni [1], Eugenio Nelson Cavallari [1], Francesca Lombardi [5], Alessandra Piccirilli [6], Stefano Fiorucci [7], Adriana Carino [7], Silvia Marchianò [7], Chiara M. Lofaro [1], Sara Caiazzo [1], Massimo Ciccozzi [8], Carolina Scagnolari [9], Claudio Maria Mastroianni [1], Giancarlo Ceccarelli [1-10*], Gabriella d'Ettorre [1]

[1] Department of Public Health and Infectious Diseases, viale del Policlinico 155, Sapienza University of Rome, Viale del Policlinico 155, 00161 Rome, Italy. (letizia.santinelli@uniroma1.it; luca.maddaloni@uniroma1.it; eugenionelson.cavallari@uniroma1.it; chiaralofaro97@gmail.com; sara.caiazzo.biotech@gmail.com; claudio.mastroianni@uniroma1.it; giancarlo.ceccarelli@uniroma1.it; gabriella.dettorre@uniroma1.it)

[2] School of Biosciences and Veterinary Medicine, Via Circonvallazione 93/95 - 62024 Matelica (MC) University of Camerino, Matelica (MC), Italy (giacomo.rossi@unicam.it)

[3] Department of Life and Environmental Sciences - DiSVA - Marche Polytechnic University – Via Brecce Bianche, 60131, Ancona (giorgia.gioacchini@univpm.it)

[4] Department of Comparative Biomedicine and Food Science BCA - University of Padua, Agripolis, Viale dell'Università, 16 - 35020 Legnaro, Padova, Italy (ranieri.verin@unipd.it)

[5] Department of Life, Health & Environmental Sciences, University of L'Aquila, Piazzale Salvatore Tommasi 1, 67100 Coppito, L'Aquila, Italy. (francesca.lombardi@univaq.it)

[6] Department of Biotechnological and Applied Clinical Sciences, University of L'Aquila, via Vetoio, Coppito – 67100, L'Aquila, Italy (alessandra.piccirilli@univaq.it)

[7] Department of Surgical and Biomedical Medicine and Surgery Sciences, University of Perugia, Piazza Università, 1, 06123, Perugia, Italy (stefano.fiorucci@unipg.it; adriana.carino@hotmail.it; silvia4as@hotmail.it).

[8] Unit of Medical Statistics and Molecular Epidemiology, University Campus Bio-Medico of Rome, Via Alvaro Del Portillo 21, 00128, Rome, Italy. (m.ciccozzi@unicampus.it)

[9] Laboratory of Virology, Department of Molecular Medicine, affiliated to Istituto Pasteur Italia, Sapienza University, viale di Porta Tiburtina 28, 00185, Rome, Italy. carolina.scagnolari@uniroma1.it

[10] Azienda Ospedaliero-Universitaria Policlinico Umberto I, Viale del Policlinico 155, 00161 Rome, Italy (giancarlo.ceccarelli@uniroma1.it)

* Correspondence:

Giancarlo Ceccarelli, MD PhD MSc. Department of Public Health and Infectious Diseases, Sapienza University of Rome, Viale del Policlinico 155, 00161, Rome, Italy; giancarlo.ceccarelli@uniroma1.it

ABSTRACT

Background: Functional and structural damage of the intestinal mucosal barrier significantly contribute to translocation of gut microbial products into the bloodstream and are largely involved in HIV-1 associated chronic immune activation. This microbial translocation is largely due to a progressive exhaustion of intestinal macrophage phagocytic function, which leads to extracellular accumulation of microbial derived components and results in HIV-1 disease progression. This study aims to better understand whether the modulation of gut microbiota promotes an intestinal immune restoration in people living with HIV (PLWH).

Methods: Long-term virologically suppressed PLWH underwent blood, colonic and fecal sampling before (T0) and after 6 months (T6) of oral bacteriotherapy. Age- and gender-matched uninfected controls (UC) were also included. 16S rRNA gene sequencing was applied to all participants' fecal microbiota. Apoptosis machinery, mitochondria and apical junctional complex (AJC) morphology and physiological functions were analyzed in gut biopsies.

Findings: At T0, PLWH showed a different pattern of gut microbial flora composition, lower levels of occludin (p=0.002) and zonulin (p=0.01), higher Claudin-2 levels (p=0.002), a reduction of mitochondria number (p=0.002) and diameter (p=0.002), as well as increased levels of LPS (p=0.018) and cCK18 (p=0.011), compared to UC. At T6, an increase in size (p=0.005) and number (p=0.008) of mitochondria, as well as amelioration in AJC structures (p<0.0001) were observed. Restoration of bacterial richness (Simpson index) and biodiversity (Shannon index) was observed in all PLWH receiving oral bacteriotherapy

(p<0.05). Increased mitochondria size (p=0.005) and number (p=0.008) and amelioration of AJC structure (p<0.0001) were found at T6 compared to T0. Moreover, increased occludin and zonulin concentration were observed in PLWH intestinal tracts and decreased levels of Claudin-2, LPS and cCK18 were found after oral bacteriotherapy (T0 vs T6, p<0.05 for all these measures).

Interpretation: Oral bacteriotherapy supplementation might restore the balance of intestinal flora and support the structural and functional recovery of the gut mucosa in antiretroviral therapy treated PLWH.

1 INTRODUCTION

HIV-1 infection is associated with a damage of intestinal epithelium, translocation of commensal bacteria and their metabolic products into the bloodstream and, ultimately, with a condition of chronic immune activation. The most relevant mechanisms underlying gut mucosal damage are represented by apoptosis of enterocytes, structural alteration of the tight junction and massive depletion of mucosal CD4 T-cells[1].

The extent of systemic translocation of gut-derived microbial products correlates with the magnitude of epithelial breakdown[2] and is largely dependent on the dynamics of macrophage phagocytosis activity in the lamina propria[3]. A progressive exhaustion of intestinal macrophage phagocytic function with extracellular accumulation of microbial components, is largely involved in the pathogenesis of HIV-associated microbial translocation. A complex chain of events that involves caspase-cleaved keratin 18 (cCK-18) driven enterocytes modifications, mucosal immune dysfunction, damage of barrier function of the intestinal epithelia, microbial translocation and chronic systemic immune activation, all ultimately contribute to disease progression[4,5] (Figure 1). It has been demonstrated that structural and functional damage of the intestinal mucosal barrier and local immune disfunction result in an increased permeability of the gut mucosa[6-10] with a subsequent systemic translocation of bioactive microbial products that can trigger immune activation

and ultimately represent the cause and effect of disease progression[10]. In fact, increased plasma concentrations of LPS have been described as a reliable marker of microbial translocation and, hence, of gut permeability[11]. Additionally, zonulin is considered an essential regulator of tight junction function gut epithelium as well as vascular endothelium[12].

Knowing that cell-cell adhesion ensures an effective physical anchorage system to preserve highly organized and stable tissue structure, mucosal barrier function cannot be maintained without a strictly regulated pattern of multiple protein structures, overall identified as apical junctional complexes (AJC), which include tight junctions (TJs), adherent junctions and desmosomes[13,14]. In enterocytes, TJs are located on the apical side of the cell membrane and regulate paracellular permeability. TJs consist of four integral proteins: occludin, claudins, junctional adhesion molecule (JAM) and tricellulin[15]. The neighboring cells participate to the barrier structure trough the activity of complex proteins located in the cytosol, like the zonula occludens (ZO) which binds the transmembrane proteins to the junctional actomyosin ring. Similarly, e-cadherin is primarily involved in the adherent junctions trough the interaction with actin cytoskeleton and plays a crucial role in structural and functional homeostasis of healthy epithelial tissue[15]. In a previously published paper[10], we showed that administration of probiotics promotes the recovery of the intestinal homeostasis in PLWH on effective antiretroviral therapy (ART), providing a potential long term benefit in addition to the central role of ART[10,16-18]. In the attempt to better understand the potential benefits of oral bacteriotherapy in PLWH, this study aims to determine whether the supplementation with high concentration of a multi-strain probiotic mixture promotes the structural and functional restoration of gut mucosa integrity. Our investigation focuses on the evaluation of cellular morphology, activation of cellular apoptosis machinery, mitochondrial and AJC restoration in PLWH and uninfected controls.

2   MATERIAL AND METHODS

Study design, recruitment, and study eligibility criteria

In this pilot study, 10 effectively ART treated men LWH and five gender- and age matched uninfected controls (UC) were recruited at the Department of Public Health and Infectious Diseases of "Sapienza" University of Rome (Italy). The inclusion criteria were as follows: (i) male sex; (ii) ≥18 years old; (iii) receiving ART treatment; (iv) plasma HIV-1 RNA <37

copies/mL and CD4+ T counts >400 cells/mm^3. Exclusion criteria included: (i) known or suspected allergy or intolerance to the specific probiotic formulation; (ii) use of probiotics or antibiotics during the 3 weeks prior to enrollment; (iii) history of illegal drug abuse; (iv) history of or current inflammatory diseases of the small or large intestine; (v) diarrhea; (vi) any current, past, or systemic malignancy; (vii) pregnancy. Patients received oral supplementation with a lyophilized multistrain probiotic supplement (*Lactobacillus plantarum* DSM24730, *Streptococcus thermophilus* DSM24731, *Bifidobacterium breve* DSM24732, *L. paracasei* DSM24733, *L. delbrueckii subsp. bulgaricus* DSM24734, *L. acidophilus* DSM 24735, *B. longum* DSM24736, *B. infantis* DSM24737), twice a day for 6 months (total daily dosage of $1.8x10^{12}$ live bacteria) [19].The study was approved by the institutional review board (Department of Public Health and Infectious Diseases, Sapienza, University of Rome) and institutional Ethics Committee (Sapienza, University of Rome). All study participants signed written informed consent. No adverse event was observed during the follow-up and all subjects maintained undetectable plasma viral load (HIV-1 RNA < 37 copies/mL) during the course of probiotic supplementation.

Laboratory procedures

All HIV positive participants underwent blood sample collection and complete colonoscopy with biopsies at baseline (T0) and after 6 months (T6) of probiotic supplementation, as previously reported[10]. Fecal samples were also collected (2 to 3 g) at T0 and T6 and stored at -80°C. Uninfected controls underwent the same procedures, with the exemption of T0 fecal sampling.

16S rRNA sequencing

Microbial DNA was purified from fecal samples using PureLink Microbiome DNA Purification Kit (Thermo Scientific™) following the manufacturer's instructions and then quantified with a Qubit dsDNA HS Assay Kit on Qubit 3.0 fluorometer (Thermo Scientific™). Sequencing was performed using an Ion 16S Metagenomics Kit (Thermo Scientific™) on the Ion Torrent S5 platform (Thermo Scientific™), as previously described [20].

Virological analysis

HIV-1 RNA copy number was measured in plasma by using Versant kPCR (Siemens Healthcare Diagnostic, Inc., Tarrytown, NY), with a lower limit of detetion of 37 HIV-1 RNA copies/mL.

Serological evaluation of zonulin levels, LPS, and cCK18

Twenty milliliters of whole blood were collected under fasting conditions by venipuncture in Vacutainer tubes containing ethylene-diamine-tetra-acetic acid (EDTA) (BD Biosciences, San Jose, CA) at each study visit. Plasma was separated by centrifugation and stored at -80°C for further analysis. Serological evaluation included quantification of plasma concentration of zonulin, lipopolysaccharide (LPS) and cleaved Cytokeratin 18 (cCK18) at T0 and T6. Plasma levels of zonulin were evaluated trough a commercially available enzyme-linked immunosorbent assay (ELISA) kit (Catalog number 30-ZONSHU-E01; ALPCO, Salem, NH), according to the manufacturers' protocol. Similarly, LPS plasma levels were measured using commercially available kits from Cusabio (Wuhan, China, Cat#CSB-E09945h), following the manufacturer's instructions. Absorptions were measured at 450 nm with a GloMax®-Multi+ Microplate Multimode Reader (Promega Corporation, Madison, United States). Concentrations in each sample were calculated from the standard curve, obtained by plotting absorbance *vs* known standard concentrations. Levels of cCK18 were determined using M30-Apoptosense ELISA (Peviva, Sweden), according to the manufacturer's instructions.

Histological analysis

Intestinal biopsies were fixed in 10% neutral buffered formalin (Sigma, Milan, Italy). Serial sections, 3-4 μm thick, were stained with hematoxylin and eosin (H&E) for histopathological evaluations. (4 sections for each biopsy). Sections of different intestinal tracts were digitized with the aid of a slide scanner (Panoramic SCAN II, 3DHISTECH, Budapest, Hungary) using 20x magnification and visualized with Case Viewer software (3DHISTECH, Budapest, Hungary). The pathologist blindly performed all the measurements in quadruplicate (total inflammatory cells counts, evaluation of different cellular sub-types infiltrating the intestinal mucosa, total mucosal thickness, glandular length, morphology of intestinal villi) evaluating ten appropriate fields in each of the four slides (total of 40 images per biopsy). The average value between the four sets of

measurements was used for statistical analysis. Histological variables (i.e different types of inflammatory cells, etc.) were graded according to the Updated Sydney System visual analogue scale to generate a score (0 = absent, 1 = mild, 2 = moderate, 3 = marked or severe)[21]. In particular, histological examination included assessment of inflammation by scoring the number of inflammatory cells (mononuclear cells, lymphocytes, plasma cells, and neutrophils) at a magnification of 400x HPFs. The number of inflammatory cells was evaluated by using a visual analogue scale, modified for intestinal specimens, and results were reported as the mean for the entire specimen[22]. Different degrees of inflammatory cell infiltration were scored based on the method described by Dixon et al[17] (Supplementary Materials).**Immunohistochemical evaluation**

Levels of occludin, zonulin, e-cadherin and claudin-2 expression, quantified in selected compartments of the GI tract (terminal ileum: villi, basal crypt area, villus-crypt junction; cecum, ascending colon, transverse colon and descending colon: apical crypt area, basal crypt area) were analyzed as follows: paraffin-embedded sections were processed according to antibody producers' instructions and incubated overnight with the following primary antibodies: Polyclonal rabbit anti-Claudin-2, (PAD: MH44, RRID:AB_2533911, Invitrogen Ltd., Paisley, UK), Polyclonal rabbit anti-Occludin (PAD: Z-T22, RRID: AB_2533977 Invitrogen Ltd., Paisley, UK), Monoclonal mouse anti-E-cadherin IgG2α (clone: 36, (RRID: AB_2738654, BD Biosciences, Oxford, UK) and Polyclonal rabbit anti-Zonulin (LS-C132998, LSBio Inc., USA). Subsequently, slides were incubated with biotinylated secondary antibodies, a goat anti-rabbit immunoglobulin (E0432, RRID:AB_2313609, Dako, Glostrup, Denmark) used for anti-Claudin-2, Occludin and Zonulin, while a goat polyclonal anti-mouse immunoglobulin (E 0443, RRID: AB_2687905, Dako, Glostrup, Denmark) for anti-E-cadherin. All cellular specific markers were evaluated using a light microscope (Carl Zeiss, Jena, Germany), at 40x and 10x magnification with the support of a squared eyepiece graticule (10×10 squares, total area 62,500 μm^2). Stained tissue sections were evaluated at 200x and 630x magnification to identify areas of consistent staining and acceptable orientation, as described elsewhere[18].Ten appropriate fields were chosen for each compartment and means were calculated for each intestinal region. AJC molecules positive cells were counted per section and results were expressed as IHC positive cells per 62,500 μm^2. Specifically, at least 4 consecutive sections of the same biopsy sample were adhered to each slide. Each section was subsequently stained with antibodies specific for each protein

of the AJC. For the comparative evaluation of the expression of different junction proteins, the same microscopic field was photographed after each staining, in order to evaluate how the different proteins were expressed in the same field. Aligning of the images obtained after each immunostaining from the same region of the section allowed the simultaneous mapping of the spatial distribution of all five AJC proteins probed. At the end of the count of the immune-stained cell for each protein tested, it was possible to understand on the same microscopic field how many cells were simultaneously positive for all the protein of the junctional complex tested (respectively occludin, zonulin, e-cadherin and claudin-2). Cells on sections margins were not considered for evaluation to avoid inflation of positive cells number.

TUNEL for apoptosis evaluation

For the *in situ* detection of epithelial and lymphocytes apoptosis, terminal deoxynucleotidyl transferase-mediated digoxigenin-deoxyuridine triphosphate nick-end labeling (TUNEL) was performed on histological sections of endoscopic ileal and colonic biopsy specimens collected from all HIV-1-positive patients[23,24]. Sections were digested with proteinase K treatment, 20 mg/mL (Sigma Chemical, St Louis, MO) for 15 min at RT. After digestion, sections were washed in tap water. Endogenous peroxidase activity was quenched with 3% hydrogen peroxidase for 20 min and then washed in PBS. After equilibration, sections were incubated at 37°C in a humidified chamber for 1 h in terminal deoxynucleotidyl transferase (TdT) enzyme and then placed in stop/wash buffer for 30 mins. The sections were rinsed in PBS and treated with antidigoxigenin peroxidase for 30 mins in a humidified chamber. Color on apoptotic nuclei was developed using diaminobenzidine and hydrogen peroxide for 1–3 min. Finally, sections were counterstained with Harris hematoxylin. As a positive control, an ApopTag control slide was used, whereas negative control was prepared by omitting the TdT enzyme from the nucleotide mix on seriate sections. Counts were assessed at a X200 magnification, by computer-assisted analysis and the results were expressed as median percentages of positive enterocytes inside epithelia.

Transmission electron microscopy

A fragment of each intestinal section was cut into small pieces (<1 mm^3) and fixed for 60 minutes at 48°C in periodate-lysine-paraformaldehyde fixative (PLP). Pieces of tissue were

washed three times in 50mM Sorensen's phosphate buffer, 200mM sucrose, and 100mM lysine monochlorhydrate for 20 minutes at 48°C, dehydrated through a series of ethanol washes (50%, 70%, 95%, 100%) and infiltrated with 1:1 pure ethanol: London Resin (LR) White for 60 minutes, followed by pure LRWhite, three times for 60 minutes at 48°C. Specimens were embedded in gelatin capsules filled with LRWhite and polymerized under water in 00 BEEM® capsules in the microwave using the following protocol: 10 min. with a temperature restriction at 60°C; 10 min. with a temperature restriction at 70°C, and 25 min. with a temperature restriction at 80°C. All of the ultrathin sections (<80 nm) were microtomed with an RMC MTX ultramicrotome (Elexience), placed on 200 mesh nickel grids coated with polylysine (dilution 1:1000) and stabilized for one day at RT. The sections were examined and photographed using a Jeol 1200 SX electron microscope (JEOL USA, Inc., Peabody, MA, USA). Three or four equidistant micrographs (83 × 58 μm) were taken following the profile of the mucosal epithelium of the intestinal analyzed tract, in each quadrant. For the complete TEM counting method, a montage of the entire section - intestinal epithelium profile consisting of 40-50 micrographs for each intestinal tract analyzed was performed. Each TEM micrograph was printed on 12˙5 × 12˙5 cm paper with a print magnification of 4800. The intercellular junction counts were performed manually by a single observer who was unaware of the study variables. For considering the intercellular junctions as "open" or "closed" two adjacent intact enterocyte membranes were first evaluated, with the observation of the tight junctional status just below the microvilli, followed by the adherens junctions, with the desmosomes located basolaterally (Supplementary Materials).

Mitochondrial DNA (mtDNA) quantification

For quantification of mtDNA, real-time DNA PCR analysis was performed with the NovaQUANT™ Human Mitochondrial to Nuclear DNA Ratio Kit (Novagen) according to the manufacturer's instructions. DNA extractions were performed on paraffin sections using a DNeasy Blood and Tissue Kit (Qiagen). Real-time DNA PCR were performed with the SYBR green method in a CFX96 Real-Time PCR system (Bio-Rad) using for each sample 2 ng of DNA as template. A set of four optimized PCR primer pairs targeting two mitochondrial genes (ND1 and ND6) and two nuclear genes (BECN1 and NEB) (provided by the NovaQUANT™ Human Mitochondrial to Nuclear DNA Ratio Kit (Novagen) were

used to measure the ratio of mtDNA to nuclear DNA, representing the relative mtDNA copy number, which in turn reflects the mtDNA content per cell.

Real-time PCR for Cytochrome C (CYT C), HSP 60 and 70

Total RNA extraction from paraffin embedded biopsies optimized using RNAzol RT reagent (SIGMA-ALDRICH). Final RNA concentration was determined by the NanoPhotometer P-Class (Implen). RNA integrity was verified by GelRedTM staining of 28S and 18S ribosomal RNA bands on 1% agarose gel. RNA was stored at -80°C until use. A total amount of 2 μg of RNA was used for cDNA synthesis, employing HighCapacity cDNA Reverse Transcription Kit (Bio-Rad) following the manufacturer's instructions. PCRs were performed in triplicates with the SYBR green method in a CFX96 Real-Time PCR system (Bio-Rad). Glyceraldehyde-3-phosphate dehydrogenase (GAPDH) and beta actin, (ACTB) were used as internal standards in order to standardize the results by eliminating variation in mRNA and cDNA quantity and quality, using the CFX Manager Software version 3.1 (Bio-Rad), including Genex Macro Conversion and Genex Macro files based on principles outlined by Vandesompele et al[25]. No amplification products were observed in negative controls and no primer-dimer formations were observed in the control templates as indicated by the melting curve analysis. Specific primer pairs for target genes (Table 1) were designed with Primer-Blast (RRID:SCR_003095)[26].

Statistical analysis

Statistical analyses were performed using SPSS software, version 22.00 (IBM, Somers, NY) on data obtained from peripheral blood, gut, and stool samples of PLWH before and after probiotic supplementation. Data obtained at T0 and T6 analysis in peripheral blood and intestinal districts were compared by Wilcoxon test for paired samples. The same test was also used to evaluate data obtained from stool samples at T0, T2, and T6. Results are given as medians, ranges, and percentages. P values <0.05 were considered statistically significant. All graphs were generated by using GraphPad Prism (RRID:SCR_002798).

Role of the funding source

The funders of the study had no role in study design, data collection, data analysis, data interpretation, and writing of the report.

RESULTS

Participant characteristics

The present study included 10 Caucasian men LWH, with an average age of 50 years (IQR 19), on effective long-term ART. At study enrolment, HIV-1-positive participants had a median CD4+ T cells count of 806 cells/mm^3 (IQR 158). Median CD4+ T cells nadir count was 255 cells/mm^3 (IQR 165). All HIV-1-positive subjects showed HIV-1 RNA <37 copies/mL for at least 12 months prior to enrollment and were on ART for a median of 10 years (IQR 13). As a control group, we included 5 seronegative age- and gender-matched uninfected controls with a median age of 48 years (IQR 13).

Microbiota composition changes after oral bacteriotherapy

We found that HIV positive participants had a distinct fecal microbiota composition pattern when compared to controls (Figure 1A and 1B). The most predominant phyla in both PLWH and uninfected controls were Actinobacteria, Bacteroidetes, Firmicutes, and Proteobacteria (Figure 2A). *Bifidobacteriacae* (p=0·0290) and *Ruminococcaceae* (p=0·0280) showed reduced concentration in HIV-1 infected men compared to controls (Figure 2B). Additionally, estimation of biodiversity (Shannon index: p=0·0401; Simpson index: p=0·0139) and richness [Principal Component Analysis (PCA)] showed a significant reduction in fecal microbiota diversity among HIV positive participants in comparison to controls (Figure 2C-D). Notably, PLWH receiving oral bacteriotherapy showed a significant increase in Actinobacteria (T0 vs. T6, p=0·0448), whereas representation of Bacteroidetes significantly decreased (T0 vs. T6, p=0·003; Figure 2A); on the other hand, at a family level, *Prevotellacae* showed a significant reduction (T0 vs. T6, p=0·0260), while *Coriobacteriacae* significantly increased (T0 vs. T6, p=0·0044; Figure 2B). Moreover, microbial diversity and richnes in HIV positive participants increased after six months of oral bacteriotherapy (Shannon Index: T0 vs. T6, p=0·0182; Simpson Index: T0 vs. T6, p=0·0281; Figure 2C-D). Reconstitution of microbial composition was also proved trough the comparison between uninfected controls and HIV positive participants at T6 (UC vs. T6, p<0·05 for all measurements, except for *Streptococcacae* family; Figure 2A-D).

Additionally, no differences in phylum and family were observed in fecal samples of uninfected controls at T0 and T6 (p>0˙05 for all measurements; Figure 2A-D).

Lipopolysaccharide, zonulin and cCK-18 plasma levels changes after oral bacteriotherapy

In PLWH, endogenous LPS levels were higher compared to uninfected controls before oral bacteriotherapy supplementation (p=0˙018). By contrast, at T0 a lower amount of zonulin was observed in PLWH than UC (p=0˙007 Figure 3A-B,). After six months of oral bacteriotherapy, LPS and zonulin levels in PLWH significantly increased (LPS: T0 vs. T6, p=0˙005; zonulin: T0 vs. T6, p=0˙0001;) and reached similar levels as in uninfected controls at T0 (UC vs. T6, p>0.05). Increased plasma levels of endogenous cCK-18, a marker of epithelial apoptosis[27], were found at baseline in PLWH compared to uninfected controls (p=0˙011; Figure 3C). After oral bacteriotherapy, cCK-18 levels in PLWH decreased significantly (T0 vs. T6, p=0˙005), but still remained higher than those found in uninfected controls at T0 (UC vs. PLWH T6, p=0˙0007).

Reduction of histology score and enterocytes apoptosis and improvement of epithelial integrity after oral bacteriotherapy

Histopathological evaluation of intestinal biopsies from PLWH showed higher histology scores, indicating increased inflammation compared to uninfected subjects [UC: 1 (IQR:0-1.5) vs PLWH: 7 (IQR: 5-9), p<0˙0001). After oral bacteriotherapy supplementation, no significant modification was observed in histology score among PLWH [T0: 7 (IQR: 5-9) vs. T6: 6 (IQR: 0-8), p=0˙865), and T6 histology score of PLWH remained significantly higher when compared to uninfected controls (UC vs. PLWH T6, p=0˙003). From a morphological point of view, after the administration of probiotics, sections of all tracts of intestinal mucosa, regardless of the intestinal tract examined, showed an improvement in epithelial integrity, a reduction in diffuse interstitial inflammatory infiltrate and an increase in the number and total area of the GALT structures. When then evaluated the inflammatory infiltrate in intestinal biopsies collected before and after probiotic supplementation, focusing on intraepithelial lymphocyte (IEL) density. We observed a general decline in the number of IELs in all intestinal tracts analyzed after probiotic supplementation. In particular, the number of IELs was significantly lower at T6 than T0 in cecum, ileum, and transverse

colon. Finally, we observed a strong reduction of the polymorphonuclear cells (PMNCs), which represent the "active" phase of the inflammatory infiltrate.

AJC ultrastructural state and modification after oral bacteriotherapy

The endogenous levels of occludin (p=0ˈ002) and zonulin (p=0ˈ01) were lower in gut biopsies from PLWH at baseline compared to those from UC; on the contrary, PLWH showed higher duodenal claudin-2 levels at baseline than UC (p=0.002, Figure 4), as well as in the large intestine (Figure 5, p<0.001). At T6, an increase in expression of occludin (T0 vs. T6, p=0.007) and zonulin (T0 vs. T6, p=0.005) was observed in PLWH, although that were not statistically different from uninfected controls (UC vs T6, p=0.005,). When considered separately, zonulin showed a significant reduction in the large intestine after oral bacteriotherapy in HIV infected participants (T0 vs. T6, p<0.001; Figure 5, Panel B, C). Similarly, at T6 we observed a reduction in claudin-2 expression among PLWH, although levels were still significantly higher than in uninfected controls (UC vs PLWH T6, p=0ˈ0007;). By contrast no differences in e-cadherin was observed between T0 and T6 among PLWH, nor between HIV infected participants and uninfected controls (PLWH vs. UC, p=0.27; T0 vs T6, p=0.285). While at T0 histopathology showed a faint occluding and zonulin staining on the luminal side of intestinal epithelium (Figure 4E, G), at T6 we observed increased occludin and zonulin staining at the AJC of luminal epithelium covering the apical portion of villi (T6, Figure 4F, H). By contrast, no discernible differences in the distribution or staining intensity for e-cadherin were observed in ileal mucosa before and after oral bacteriotherap in PLWH (Figure 4I, L). The overall intensity of e-cadherin staining progressively decreased from the luminal epithelium to distal crypts. Staining for claudin-2 labelling resulted most intense at the epithelial cell AJC of the luminal epithelium at the apical portion of villi in the ileum T0 biopsies from PLWH, while a weak to absent staining was observed in the luminal epithelium and in some intestinal glands of the same intestinal tract at T6 (Figure 4M, N).

Interestingly, at T0 the tight junction-like structures at the basolateral pole of enterocytes and at the apical surface of colonic cells in PLWH were in an open form, as per ultrastructural examination (Figure 6A). By contrast, after oral bacteriotherapy, gut biopsies showed a "close" aspect of the junctional complex in all analyzed participants (Figure 6B).

Ultrastructural changes in mitochondrial size and number after oral bacteriotherapy

To characterize the effect of oral bacteriotherapy supplementation on size and number of intestinal mitochondria, TEM analysis was performed on gut biopsies derived from all the examined intestinal tracts. At baseline, PLWH had a lower number (p=0˙002) and diameter (p=0˙002) of mitochondria than uninfected controls (Figure 7A-B). At T6 we observed an increase in number (T0 vs. T6, p=0˙008) and diameter of mitochondria (T0 vs. T6, p=0˙005; Figure 7A-B). However, when compared to UC, HIV infected participants showed a lower number of mitochondria (UC vs. T6, p=0˙0007); by contrast, no significant differences were observed in terms of mitochondria diameter between PLWH and UC (Figure 7A).

Changes of mtDNA, *CYT C* mRNA, *HSP60* mRNA and *HSP70* mRNA levels after six months of oral bacteriotherapy

To better define the mucosal ultrastructural modifications observed, MtDNA, *CYT C* mRNA, *HSP60* mRNA, and *HSP70* mRNA were also evaluated. At T0, a decreased gut levels of mtDNA (p=0˙005), *CYT C* mRNA (p=0˙005), *HSP60* mRNA (p=0˙01) and *HSP70* mRNA (p=0˙005) mRNA were observed in PLWH in respect to uninfected controls (Figure 8A-D). After oral bacteriotherapy, an increase in the concentrations of mtDNA (T0 vs T6, p=0˙03;), *CYT C* mRNA (T0 vs T6, p=0˙01;), *HSP60* mRNA (T0 vs T6, p=0˙04) and *HSP70* mRNA (T0 vs T6, p=0˙02) were observed (Figure 8), although without statistically significant difference in respect to uninfected controls (UC vs PLWH T6).

DISCUSSION

Our study shows that substantial alterations of fecal microbial composition can be observed in ART treated PLWH with undetectable viremia. After six months of oral bacteriotherapy supplementation, microbiota biodiversity and richness increased with a sharp reduction in the relative abundances of *Prevotellacae* and an increase in *Bifidobacteriacae*. In concordance with data obtained by TUNEL analysis we performed on gut biopsies collected after oral bacteriotherapy supplementation, plasma levels of the apoptosis marker cCK-18 were reduced in the HIV-1-positive individuals enrolled, suggesting the existence of a strong relationship between gut epithelial integrity and apoptosis of enterocytes. However, compared to uninfected controls, PLWH receiving probiotics still show higher levels of cCK-18. Futhermore, for the first time to our knowledge, we observed a probiotic-induced modulation of the expression of AJC proteins, with changes in the levels of occludin,

claudin-2 and zonulin; on the other hand we did not observe effects on e-cadherin. In our study population, oral bacteriotherapy also promoted an increase in the number and volume of IECs mitochondria, IECs mtDNA and expression levels of *cytochrome C* mRNA. Another important finding of our study was a probiotic-induced increase in the expression of HSP60 and HSP70 mRNA in the gut, as well as a decrease in endogenous levels of zonulin in plasma and gut mucosa of HIV infected individuals in comparison to controls. Overall, our results indicate that oral bacteriotherapy seems to promote microbiota homeostasis in PLWH, through a reduction of specific pathogenic bacterial taxa which are usually associated with chronic inflammatory intestinal diseases[28]. In a previously published paper[10], we observed intestinal histologic, morphologic and ultrastructural changes after oral probiotic supplementation. In particular, we showed a reduction of mucosal inflammatory infiltrate and enterocyte apoptosis in terminal ileum, cecum, ascending colon, transverse colon, and descending colon, confirming the presence of gut alterations in HIV-1-positive patients, mostly represented by villous blunting and widening, vacuolated enterocytes, crypt hyperplasia, and increased presence of inflammatory cells in the lamina propria[29].

In this context, the high persistent levels of cCK-18 that we observed could be explained in consideration to apoptosis phenomena occurring in liver or kidneys in HIV-1 infected subjects, as a direct consequence of ART toxicity[30,31].

The heterogeneous effects of this specific bacteriotherapy on the AJC, as well as on protein expression, might be partly determined by the bacterial strains that characterize the product itself[32]. Although our data showed an incomplete recovery of claudin-2 in HIV-infected patients compared to controls, it is possible that the tight junction associated membrane proteins with their distinctive activities and structure might cooperate to ensure full barrier function. Therefore, our data suggest that occludin, claudin-2 and zonulin might be sufficient to maintain the integrity of intestinal barrier. Electron microscopy studies have demonstrated that ultrastructural alterations in IECs mitochondria, such as dissolved/irregular cristae indicative of impaired function, occur early during inflammation[4]. The increase in mtDNA and cytocrome C mRNA levels highlight the recovery of a healthy mitochondria population, which is essential for crypt formation and for the function of enteric barrier. In addition, the human mitochondrial HSP70 (mtHSP70 or mortalin) represents the central mitochondrial chaperone, actively involved in the correct folding of

mitochondrial precursor proteins. Its high intra-mitochondrial expression is implied in the preservation of mitochondrial multiplication and functionality[33]. The effectiveness of this specific oral bacteriotherapy in maintaining mitochondrial functionality is supported by a correlation between the downregulation of HSP60 levels and the increased expression of IL-6 and TNF-α, produced by macrophages upon TLR or Th1 activation in adults with diabetes[34,35]. Recently, HSP70 has been shown to co-precipitate with Vpr (the viral HIV-1 R protein, which contributes to the nuclear translocation and replication process of HIV-1 in macrophages), in HIV infected subjects. When present in high concentration within cells, HSP70 competes with Vpr, efficiently inhibiting viral translocation and replication [36]. Moreover, silencing of HSP70 expression can lead to an increased HIV-1 expression and replication in 293 T cells[37]. Zonulin is synthesized by enterocytes and hepatocytes, and is considered a biomarker of intestinal permeability[38]. Zonulin is involved in the regulation of intestinal mucosal barrier and elevated plasma levels of this protein are correlated to a "*leaky gut*" condition[39]. A correlation between increased plasma levels of zonulin, sarcopenia and cognitive decline have been recently observed in subjects with Alzheimer disease[40]. Our data show that oral bacteriotherapy led to a reduction in plasma level of LPS and endogenous zonulin, thus indicating a positive effect on intestinal permeability and microbial translocation. Overall, the above evidences suggests that supplementing ART therapy with oral bacteriotherapy might induce restoration of gut microbiota and recovery of the energetic processes at the mitochondrial level. However, since differences were still present between HIV infected individuals and UC at the end of the study, we argue that a six months course of probiotic supplementation might not be sufficient to reach a complete recovery of the gastrointestinal damage. To date, few studies have examined the effects of oral bacteriotherapy on gut-mucosal barrier in the setting of HIV infection, especially with this specific probiotic formulation. Further studies are needed to investigate whether these beneficial effects are maintained over time, as well as the optimal duration of probiotic supplementation required to revert gut alterations to a situation similar to that of UC. Overall, the available data on the use of probiotics in PLWH are extremely heterogeneous, due to a multitude of different probiotic formulations, durations of treatment and measured outcomes. Therefore, it is not possible to speculate whether the effects obtained with the administration of a specific formulation to a specific kind of patients will be observed with the use any other probiotic compound. Moreover, we are aware that limitations of our analysis include the lack of a control group of HIV-1 long term suppressors untreated with

oral bacteriotherapy as well as the lack of intestinal biopsies at T6 in the uninfected controls' group, which might affect the power of the study to detect spontaneous fluctuations in intestinal microbiota composition and in junctional proteins representation. Moreover, although colonoscopy examination for obtaining multiple gut mucosa biopsies was safe and well tolerated by all participants, it is important to underline that it still represents a relatively invasive procedure.

Our next aim will be to assess whether the improvement in mitochondrial function we observed in PLWH has a clinical impact on the course of "early senescence." We have already demonstrated cognitive improvements following the administration of the same bacterial formulation that we used in the present study[41]. Our observations need to be confirmed and extended to other organs and compartments. Currently, although antiretroviral therapy has changed HIV infection into a manageable chronic disease, HIV infected individuals might suffer from mitochondrial dysfunction and "energetic crises" that can persist for the entire course of life.

CONTRIBUTORS

LS wrote the paper, carried out the experiment and performed statistical analysis. LM, FL, AP, AC, SM, CL and SC collected the samples and participated in carrying out the experiments. GC, ENC and GdE provided patient's samples and participated in the design and revision of the manuscript. CS, SF and CMM participated in the design and revision of the manuscript. GR, GG, RV, GdE equally contributed to conceive the study, analyse the data, write the paper, and supervise the work. All authors reviewed the work and approved the final manuscript.

ACKNOWLEDGMENTS

None

DECLARATION OF INTEREST

The authors declare that the research was conducted in the absence of any commercial or financial relationships that could be construed as a potential conflict of interest.

DATA AVAILABILITY AND DATA SHARING STATEMENTS

The data supporting the findings of this study are openly available in Mendeley data repository (reference number linking to the repository "Microbiota alterations in patients living with HIV", Mendeley Data, V1, doi: 10.17632/2g87td73ty.1; "Gut barrier impairment and mitochondrial dysfunction in patients living with HIV", Mendeley Data, V1, doi: 10.17632/x8t77wx8bz.1).

REFERENCES

1. Marchetti G, Tincati C. and Silvestri G. Microbial translocation in the pathogenesis of HIV infection and AIDS. *Clin Microbiol Rev*. 2013; 26(1):2-18.

2. Estes JD, Harris LD, Klatt NR, Tabb B, Pittaluga S, Paiardini, M et al. Damaged intestinal epithelial integrity linked to microbial translocation in pathogenic simianimmunodeficiency virus infections. *PLoS Pathog*. 2010; 19;6(8): e1001052.

3. Estes JD, Gordon, SN, Zeng M, Chahroudi M, Dunham RM, Staprans SI et al. Early resolution of acute immune activation and induction of PD-1 in SIV-infected sooty mangabeys distinguishes nonpathogenic from pathogenic infection in rhesus macaques. *J. Immunol*. 2008; 180:6798 –6807.

4. Douek DC, Roederer M, Koup RA. Emerging concepts in the immunopathogenesis of AIDS. *Annu. Rev. Med*. 2009; 60:471–484.

5. Paiardini M, Frank I, Pandrea I, Apetrei C, Silvestri G. Mucosal immune dysfunction in AIDS pathogenesis. *AIDS Rev.* 2008; 10:36 –46.

6. Sharpstone D, Neild P, Crane R, Taylor C, Hodgson C, Sherwood R et al. Small intestinal transit, absorption, and permeability in patients with AIDS with and without diarrhoea. *Gut*. 1999; 45(1):70-6

7. Clayton F, Kapetanovic, S, Kotler, DP. Enteric microtubule depolymerization in HIV infection: a possible cause of HIV-associated enteropathy. *AIDS.* 2001;15:123–124.

8. Kapembwa, MS, Fleming, SC, Sewankambo, N, Serwadda, D, Lucas, S, Moody, A et al. Altered small-intestinal permeability associated with diarrhoea in human-

9. Kotler, DP, Gaetz, HP, Lange, M, Klein, EB, Holt, PR. Enteropathy associated with the acquired immunodeficiency syndrome. *Ann. Intern. Med.* 1984; 101:421–428 (.

10. d'Ettorre G, Rossi G, Scagnolari C, Andreotti M, Giustini N, Serafino S et al. Probiotic supplementation promotes a reduction in T-cell activation, an increase in Th17 frequencies, and a recovery of intestinal epithelium integrity and mitochondrial morphology in ART-treated HIV-1-positive patients. *Immun Inflamm Dis*. 2017; 5(3):244-260.

11. Nowroozalizadeh S, Månsson F, da Silva Z, Repits J, Dabo B, Pereira C, et al. Microbial translocation correlates with the severity of both HIV-1 and HIV-2 infections. *J. Infect. Dis.* 2010; 201:1150–54.

12. Sturgeon, C, Fasano, A. Zonulin, a regulator of epithelial and endothelial barrier functions, and its involvement in chronic inflammatory diseases. *Tissue. Barriers.* 2016; 21;4(4):e1251384.

13. Bhat AA, Uppada S, Achkar IW, Hashem S, Yadav SK, Shanmugakonar M, et al. Tight junction proteins and signaling pathways in cancer and inflammation: a functional crosstalk. *Front Physiol.* 2018;9:1942.

14. Garcia MA, Nelson WJ, Chavez N. Cell-cell junctions organize structural and signaling networks. *Cold Spring Harb Perspect Biol*. 2018;10(4):139–148.

15. Panwar S, Sharma S and Tripathi P. Role of Barrier Integrity and Dysfunctions in Maintaining the Healthy Gut and Their Health Outcomes. *Front. Physiol.* 2021;12:715611.

16. Ganji-Arjenaki M, and Rafieian-Kopaei M. Probiotics are a good choice in remission of inflammatory bowel diseases: a meta analysis and systematic review. *J. Cell Physiol.* 2018; 233(3):2091-2103.

17. Gionchetti, P, Rizzello, F, Venturi, A, and Campieri, M. Probiotics in infective diarrhoea and inflammatory bowel diseases. *J. Gastroenterol. Hepatol*. 2000; 15:489–493.

18. Rossi, G, Pengo, G, Caldin, M, Palumbo Piccionello, A, Steiner, JM, Cohen, ND, et al. Comparison of microbiological, histological, and immunomodulatory parameters in response to treatment with either combination therapy with prednisone and metronidazole or probiotic strains in dogs with idiopathic inflammatory bowel disease. *PLoS ONE.* 2014; 10;9(4): e94699.

19. Scagnolari, C Corano Scheri, G, Selvaggi, C, Schietroma, I, Najafi Fard, S, Mastrangelo,A et al. Probiotics Differently Affect Gut-Associated Lymphoid Tissue Indolamine-2,3- Dioxygenase mRNA and Cerebrospinal Fluid Neopterin Levels in Antiretroviral-Treated HIV-1 Infected Patients: A Pilot Study. *Int J Mol Sci.* 2016; 17(10).

20. Biagioli M, Capobianco D, Carino A, Marchianò S, Fiorucci C, Ricci P, et al. Divergent Effectiveness of Multispecies Probiotic Preparations on Intestinal Microbiota Structure Depends on Metabolic Properties. *Nutrients.* 2019;11(2):325.

21. Dixon, MF, Genta, RM, Yardley, JH, Correa, P. Classification and grading of gastritis. The updated Sydney System. International Workshop on the Histopathology of Gastritis, Houston 1994. *Am. J. Surg. Pathol.* 1996; 20:1161–1181.

22. IBD Working Group of the European Society for Paediatric Gastroenterology, Hepatology and Nutrition. Inflammatory bowel disease in children and adolescents: recommendations for diagnosis-the Porto criteria. *J. Pediatr. Gastroenterol. Nutr.* 2005; 41:1–7.

23. Gavrieli, Y, Sherman, Y, and Ben-Sasson, SA. Identification of programmed cell death in situ via specific labeling of nuclear DNA fragmentation. *J. Cell Biol.* 1999; 119:493–501.

24. Ciccocioppo, R, Di Sabatino, A, Parroni, R, Muzi, P, D'Alò, S, Ventura, T, et al. Increased enterocyte apoptosis and Fas-Fas ligand system in celiac disease. *Am. J. Clin. Pathol.* 2001; 115:494–503.

25. Vandesompele J, De Preter K, Pattyn F, Poppe B, Van Roy N, De Paepe A et al. Accurate normalization of real-time quantitative RT-PCR data by geometric averaging of multiple internal control genes. *Genome Biol.* 2002, 3, research0034.1

26. Ye J, Coulouris, G, Zaretskaya, I, Cutcutache, I, Rozen, S, Madden, TL. Primer-BLAST: a tool to design target-specific primers for polymerase chain reaction. *BMC Bioinformatics* 2012; 13, 134.

27. Hoffmanová I, Sánchez D, Hábová V, Anděl M, Tučková L, Tlaskalová-Hogenová H. Serological markers of enterocyte damage and apoptosis in patients with celiac disease, autoimmune diabetes mellitus and diabetes mellitus type 2. *Physiol Res.* 2015; 64(4):537-46.

28. Scher JU, Sczesnak A, Longman RS, Segata N, Ubeda C, Bielski C, et al. Expansion of intestinal *Prevotella copri* correlates with enhanced susceptibility to arthritis. *eLife* 2013; 2:e01202.

29. Pellecchia P, Brandt LJ. Intestinal abnormalities in AIDS. In: Classen M, Tytgat GNJ, Lightdale CJ, editors. *Gastroenterological Endoscopy*. 2010; pp. 753–765; 2nd edition. Stuttgart, Germany: Thieme.

30. Bantel H, Lügering A, Heidemann J, Volkmann X, Poremba C, Strassburg CP, et al. Detection of apoptotic caspase activation in sera from patients with chronic HCV infection is associated with fibrotic liver injury. *Hepatology*. 2004; 40:1078–1087.

31. Fischer S, Cassivi SD, Xavier AM, Cardella JA, Cutz E, Edwards V, et al. Cell Death in Human Lung Transplantation: Apoptosis Induction in Human Lungs During Ischemia and After Transplantation. *Ann. Surg.* 2000; 231(3):424-31.

32. Hummel S, Veltman K, Cichon C, Sonnenborn U, Schmidt MA. Differential Targeting of the E-Cadherin/β-Catenin Complex by Gram-Positive Probiotic

Lactobacilli Improves Epithelial Barrier Function. *Appl. Environ. Microbiol.* 2012; 78(4):1140-7.

33. Havalová H, Ondrovičová G, Keresztesová B, Bauer JA, Pevala V, Kutejová E, et al. Mitochondrial HSP70 Chaperone System-The Influence of Post-Translational Modifications and Involvement in Human Diseases. *Int J Mol Sci.* 2021;22(15):8077.

34. Moebius JS, Groos S, Meinhardt A, Seitz J. Differential distribution of the mitochondrial heat-shock protein 60 in rat gastrointestinal tract. *Cell. Tissue. Res.* 1997; 287:343–350.

35. Khadir A, Kavalakatt S, Cherian P, Warsame S, Abubaker JA, Dehbi M, et al. Physical Exercise Enhanced Heat Shock Protein 60 Expression and Attenuated Inflammation in the Adipose Tissue of Human Diabetic Obese. *Front Endocrinol (Lausanne).* 2018; 6; 9:16.

36. Iordanskiy S, Zhao Y, DiMarzio P, Agostini I, Dubrovsky L, Bukrinsky M. Heat-shock protein 70 exerts opposing effects on Vpr-dependent and Vpr-independent HIV-1 replication in macrophages. *Blood* 2004;104:1867–1872.

37. Kumar M, Rawat P, Khan SZ, Dhamija N, Chaudhary P, Ravi DS et al. Reciprocal regulation of human immunodeficiency virus-1 gene expression and replication by heat shock proteins 40 and 70. *J Mol Biol.* 2011; 410(5):944-958.

38. Moreno-Navarrete JM, Sabater M, Ortega F, Ricart W, Fernández-Real JM. Circulating zonulin, a marker of intestinal permeability, is increased in association with obesity-associated insulin resistance. *PLoS One.* 2012;7(5):e37160.

39. Fasano A. All disease begins in the (leaky) gut: role of zonulin-mediated gut permeability in the pathogenesis of some chronic inflammatory diseases. *F1000Res.* 2020 Jan 31;9:F1000 Faculty Rev-69.

40. Ogawa Y, Kaneko Y, Sato T, Shimizu S, Kanetaka H, Hanyu H. Sarcopenia and Muscle Functions at Various Stages of Alzheimer Disease. *Front Neurol.* 2018;9:710.

41. Ceccarelli G, Brenchley JM, Cavallari EN, Scheri GC, Fratino M, Pinacchio C. et al. Impact of High-Dose Multi-Strain Probiotic Supplementation on Neurocognitive Performance and Central Nervous System Immune Activation of HIV-1 Infected Individuals. *Nutrients.* 2017; 9(11):1269.
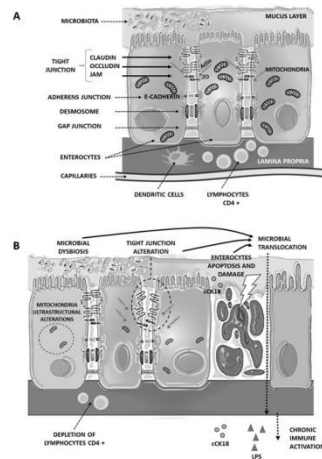
FIGURE AND TABLE LEGENDS

Figure 1. Schematic of the intestinal epithelial barrier structure in UC (A) and PLWH (B).

The highly diversified microbiota in UC resides in the gut lumen and the structural integrity maintained by epithelial cells junctions (Tight junctions, adherens junctions and desmosomes) and gut-resident immune cells function prevent the translocation of microbial species and products to the peripheral blood (A). Tight junctions are located on the apical side of epithelial cell membrane and; they are made up of some integral proteins, Occludin, Claudins and junctional adhesion molecule (JAM). E-cadherin is primarily involved in formation of adherens junction, building an interaction with actin containing cytoskeleton. Complex proteins in the cytosol, like zonula occludens (ZO) further binds the transmembrane proteins to the internal junctional actomyosin ring. Measurements of Occludin and Claudins can be used to assess paracellular permeability; E-cadherin allow the determination of cell-cell adhesion. Zonulin is considered a candidate biomarker of intestinal permeability.

Microbial dysbiosis can occur during HIV-1 Infection (B) with the extracellular accumulation of microbial components. The intestinal epithelial barrier results extremely damaged as a consequence of enterocytes modifications and apoptosis (confirmed by

increased cCk18 peripheral levels). Accordingly tight junction structures are deeply altered, with a significant variation in the occludin and claudin integral proteins levels. Enterocytes are also functionally compromised since mitochondria number and diameters are significantly reduced, thus reducing energetic processes. All these events contribute to increased microbial translocation, with higher plasma levels of LPS and chronic immune activation, both contributing to HIV-1 disease progression.

FIGURE 2 A
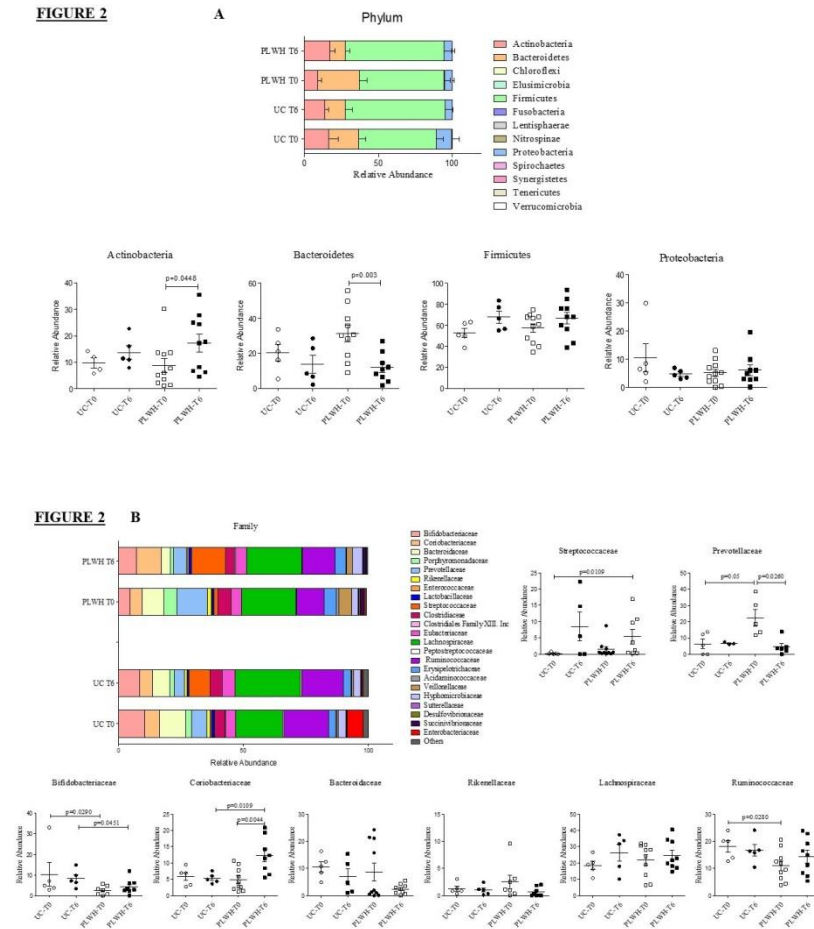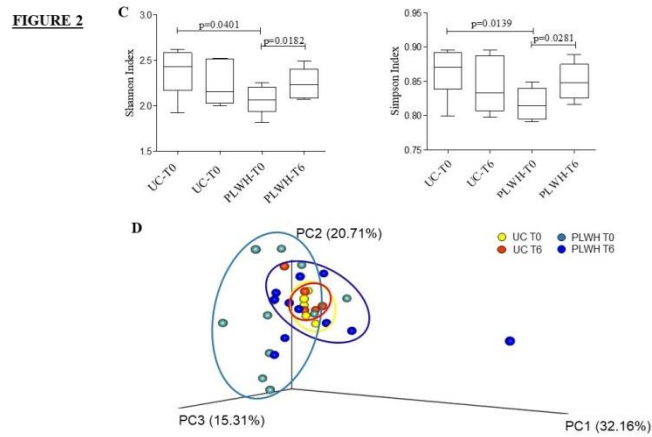
FIGURE 2 B

Figure 2. Microbiota compositional analysis in PLWH following 6 months of oral bacteriotherapy and in uninfected controls

Stacked bar plot depicting relative abundances of phyla and families in the fecal samples of PLWH before and after oral bacteriotherapy treatment and in uninfected controls (A, B). Dot Plots representing relative abundance of top abundant phyla and families (A, B) in PLWH before and after oral bacteriotherapy treatment (T0 vs T6, p<0.05, Mann-Whitney t-test) and in uninfected controls (PLWH vs HC, p<0.05, Mann-Whitney t-test). Shannon and Simpson indices were used to estimate the α-diversity among PLWH following 6 months of bacteriotherapy and uninfected controls (C). Principal Component Analysis (PCA) (for β diversity) based on the relative abundances of mapped reads/OTUs between PLWH before and after bacteriotherapy supplementation and uninfected controls (D). p<0.05 was considered to be significant.
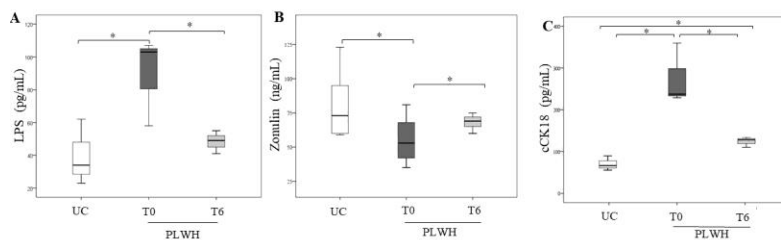
FIGURE 3

Figure 3. Differences in plasma levels of LPS, Zonulin and cCK18 in PLWH before and after oral bacteriotherapy supplementation and in uninfected controls

Plasma levels of LPS, Zonulin and cCK18 in PLWH and UC were presented as the median (horizontal bar within boxes), 25-75 percentile (upper and lower margin boxes) and range (horizontal bar above or below boxes). Data were analyzed using the Mann–Whitney test for unpaired samples (PLWH vs UC) and Wilcoxon test for paired samples (T0 vs T6). * $p < 0.05$.
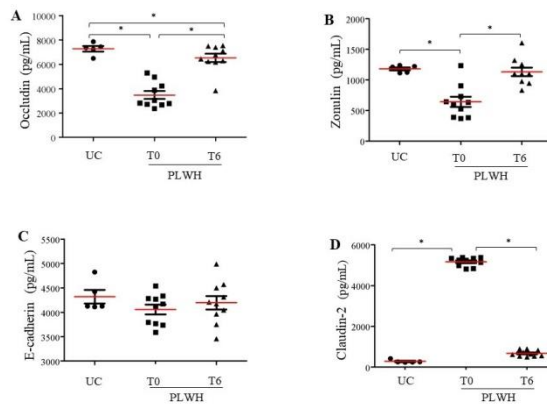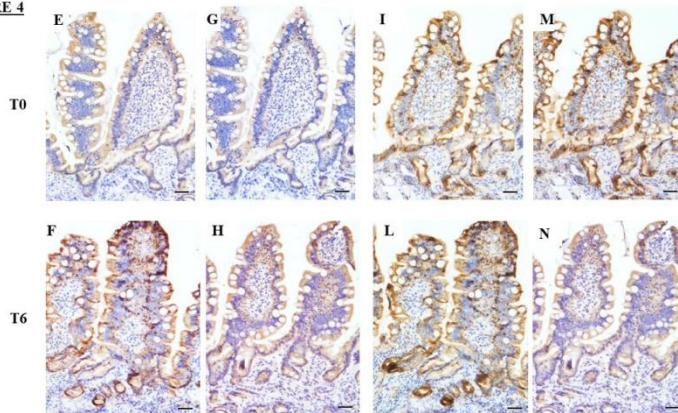
FIGURE 4

FIGURE 4

Figure 4. Expression of AJC proteins in the intestinal mucosa of PLWH and uninfected controls before and after oral bacteriotherapy treatment

Levels of Occludin, Zonulin levels Claudin-2 and E-cadherin were represented as scatter dot plot for PLWH and UC. In duodenal samples belonging to pre- and post-treated PLWH: figures E-F (and relative graph A) show the diffusion and intensity of Occludin expression. In the consecutive (adjacent) histological sections, the expression of Zonulin (G and H, graph B), of E-cadherin (I and L, graph C) and of Claudin-2 (M - N, Graph D) are shown respectively. The histological sections were randomly selected from one of the patients of the PLWH group, where immunohistochemical labeling was performed on consecutive

sections, in order to compare the localization and intensity of expression on a similar (almost identical) morphological image. of each selected protein/antigen. Each individual is represented by a distinct symbol and Median values are represented with a red horizontal line. Data were analyzed using the Mann–Whitney test for unpaired samples (PLWH vs UC) and Wilcoxon test for paired samples (T0 vs T6). * p<0.05.
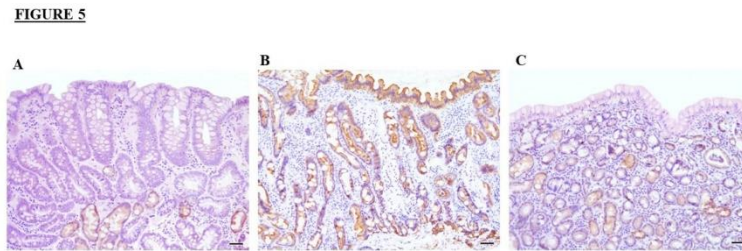
FIGURE 5

Figure 5. Comparison between the trend of expression AJC in PLWH before and after oral bacteriotherapy and uninfected controls

Colonic mucosal biopsies were evaluated before (T0) and after oral bacteriotherapy treatment (T6)(B and C) and compared to mucosal samples from uninfected controls (A). Unlike duodenal biopsies, in colon biopsies, Claudin-2 is readily detectable only in the colonic crypt epithelium, of pre-treated PLWH, but not in UC and in post treated PLWH. For the other ACJ proteins (Occludin, Zonulin, and E-Cadherin) the trend in the colon was comparable to that described in the duodenum. As for the duodenal sections, the histological sections of the colon were randomly selected from one of the patients of the PLWH group, and from a patient of the UC group, where immunohistochemical labeling was performed on consecutive sections.
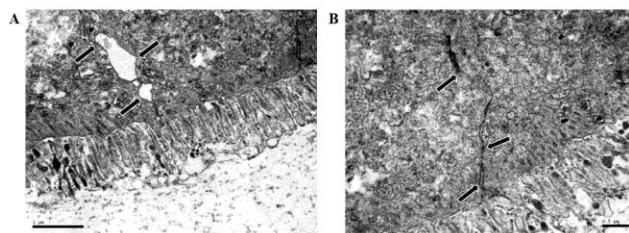
FIGURE 6

Figure 6. Transmission electron microscopy of AJC in enterocytes of PLWH before (A) and after (B) oral bacteriotherapy treatment

A)Tight junction-like structures close to the basolateral pole of enterocytes (arrows) or detected at the intercellular contact sites close to the apical surface of the colonic cells before the oral bacteriotherapy treatment. B) Junctional complex, with a reinforce of both the adjacent cellular membranes (arrows), in intestinal colonic mucosa of PLWH post oral bacteriotherapy treatment. Scale bars: 1µm (A), and 0.5µm (B)
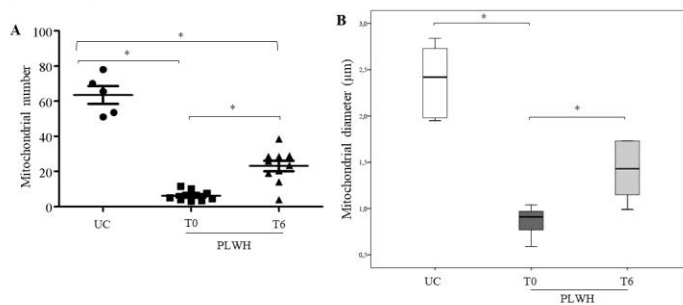
FIGURE 7

Figure 7. Transmission electron microscopy of mitochondrial number and size in enterocytes of PLWH before and after oral bacteriotherapy treatment and in uninfected controls

Mitochondrial numbers were represented as scatter dot plot for both PLWH and UC. Data for each individual were represented by a distinct symbol and median values were indicated with a red horizontal line. Mitochondrial size were presented as the median (horizontal bar

within boxes), 25-75 percentile (upper and lower margin boxes) and range (horizontal bar above or below boxes). Data were analyzed using the Mann–Whitney test for unpaired samples (PLWH vs UC) and Wilcoxon test for paired samples (T0 vs T6). * p<0.05.
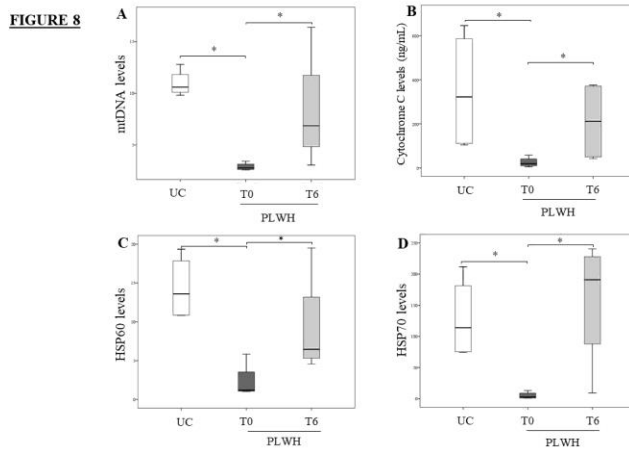

Figure 8. mtDNA, CytC, HSP60 and 70 levels in mucosal biopsies of PLWH **before and after oral bacteriotherapy treatment and in uninfected controls**

mtDNA levels (A), Cytocrome C (B), HSP60 (C) and HSP70 (D) mRNA levels were presented as the median (horizontal bar within boxes), 25-75 percentile (upper and lower margin boxes) and range (horizontal bar above or below boxes) of the relative number of copies. Data were analysed using the Mann–Whitney U test (* p<0.05).

Table 1: Real time PCR primers for CYT C, HSP 60 and 70 quantification from biopsies RNA

Gene	Forward	Reverse	Gene ID
GAPDH	GTCTCCTCTGACTTCAACAGCG	ACCACCCTGTTGCTGTAGCCAA	NM_001256799
ACTB	CACCATTGGCAATGAGCGGTTC	AGGTCTTTGCGGATGTCCACGT	NM_001101
HSP70	ACCTTCGACGTGTCCATCCTGA	TCCTCCACGAAGTGGTTCACCA	NM_005345
HSP60	TGCCAATGCTCACCGTAAGCCT	AGCCTTGACTGCCACAACCTGA	NM_002156
CYCS	AAGGGAGGCAAGCACAAGACTG	CTCCATCAGTGTATCCTCTCCC	NM_018947

IL1B	CCACAGACCTTCCAGGAGAATG	GTGCAGTTCAGTGATCGTACAGG	NM_000576
HP	TGGCTATGTGGAGCACTCGGTT	CAGGAAGTTTATCTCCAACAGCC	NM_005143